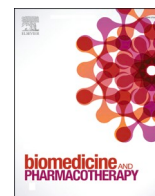




Since January 2020 Elsevier has created a COVID-19 resource centre with free information in English and Mandarin on the novel coronavirus COVID-19. The COVID-19 resource centre is hosted on Elsevier Connect, the company's public news and information website.

Elsevier hereby grants permission to make all its COVID-19-related research that is available on the COVID-19 resource centre - including this research content - immediately available in PubMed Central and other publicly funded repositories, such as the WHO COVID database with rights for unrestricted research re-use and analyses in any form or by any means with acknowledgement of the original source. These permissions are granted for free by Elsevier for as long as the COVID-19 resource centre remains active.



Identification of phytochemicals in Qingfei Paidu decoction for the treatment of coronavirus disease 2019 by targeting the virus-host interactome

Yuyun Li^{a,c,1}, Yan Wu^{b,1}, Siyan Li^{e,1}, Yibin Li^a, Xin Zhang^a, Zeren Shou^a, Shuyin Gu^a, Chenliang Zhou^a, Daohua Xu^c, Kangni Zhao^a, Suiyi Tan^a, Jiayin Qiu^{d,*}, Xiaoyan Pan^{b,*}, Lin Li^{a,*}

^a NMPA Key Laboratory for Research and Evaluation of Drug Metabolism, Guangdong Provincial Key Laboratory of New Drug Screening, School of Pharmaceutical Sciences, Southern Medical University, Guangzhou 510515, China

^b State Key Laboratory of Virology, Wuhan Institute of Virology, Center for Biosafety Mega-Science, Chinese Academy of Sciences, Wuhan 430071, China

^c Key Laboratory of Traditional Chinese Medicine and New Pharmacy Development, Guangdong Medical University, Dongguan 523808, China

^d School of Pharmaceutical Science, Zhejiang Chinese Medical University, Hangzhou 310053, China

^e School of Basic Medical Sciences, Guangzhou University of Chinese Medicine, Guangzhou 510006, China

ARTICLE INFO

Keywords:

COVID-19
Qingfei Paidu Decoction
SARS-CoV-2
Bioinformatics
Systematic pharmacology
Virus-host interactome

ABSTRACT

Qingfei Paidu decoction (QFPDD) has been clinically proven to be effective in the treatment of coronavirus disease 2019 (COVID-19). However, the bioactive components and therapeutic mechanisms remain unclear. This study aimed to explore the effective components and underlying mechanisms of QFPDD in the treatment of COVID-19 by targeting the virus-host interactome and verifying the antiviral activities of its active components in vitro. Key active components and targets were identified by analysing the topological features of a compound-target-pathway-disease regulatory network of QFPDD for the treatment of COVID-19. The antiviral activity of the active components was determined by a live virus infection assay, and possible mechanisms were analysed by pseudotyped virus infection and molecular docking assays. The inhibitory effects of the components tested on the virus-induced release of IL-6, IL-1 β and CXCL-10 were detected by ELISA. Three components of QFPDD, oroxylin A, hesperetin and scutellarin, exhibited potent antiviral activities against live SARS-CoV-2 virus and HCoV-OC43 virus with IC₅₀ values ranging from 18.68 to 63.27 μ M. Oroxylin A inhibited the entry of SARS-CoV-2 pseudovirus into target cells and inhibited SARS-CoV-2 S protein-mediated cell-cell fusion by binding with the ACE2 receptor. The active components of QFPDD obviously inhibited the IL-6, IL-1 β and CXCL-10 release induced by the SARS-CoV-2 S protein. This study supports the clinical application of QFPDD and provides an effective analysis method for the in-depth study of the mechanisms of traditional Chinese medicine (TCM) in the prevention and treatment of COVID-19.

Abbreviations: ACE2, Angiotensin-converting enzyme 2; CCK-8, Cell counting kit-8; COVID-19, Coronavirus disease 2019; CQ, Chloroquine; CC₅₀, Half-maximal cytotoxic concentration; CXCL-10, C-X-C motif chemokine ligand 10; DA, Daidzein; DEGs, Differentially expressed genes; DMSO, Dimethyl sulfoxide; GEO, Gene Expression Omnibus; GO, Gene Ontology; HE, Hesperetin; HR1, Heptad repeat 1; HR2, Heptad repeat 2; IC₅₀, Half-maximal inhibitory concentration; HCoV-OC43, Human Coronavirus OC43; IL-6, Interleukin-6; IL-1 β , Interleukin-1 β ; IS, Isoliquiritigenin; LU, Luteolin; KEGG, Kyoto Encyclopedia of Genes and Genome; NA, Naringenin; NP, Nucleoprotein; OA, Oroxylin A; OD, Optical density; PMA, Phorbol 12-myristate 13-acetate; PsV, Pseudovirus; QFPDD, Qingfei Paidu Decoction; RT-PCR, Real-time PCR; RE, Resveratrol; RRA, Robust Rank Aggregation; SARS-CoV-2, Severe acute respiratory syndrome coronavirus 2; S, Spike; SC, Scutellarin; TCM, Traditional Chinese Medicine; TCMSP, Traditional Chinese Medicine System Pharmacology Database; TE, Tectorigenin; TMPRSS2, Transmembrane serine protease 2; WO, Wogonin; 6-HB, six-helical bundle.

* Corresponding authors.

E-mail addresses: jiayinqiu@hotmail.com (J. Qiu), panxy@wh.iov.cn (X. Pan), li75lin@smu.edu.cn (L. Li).

¹ These authors contributed equally to this work.

<https://doi.org/10.1016/j.bioph.2022.113946>

Received 9 August 2022; Received in revised form 25 October 2022; Accepted 28 October 2022

Available online 31 October 2022

0753-3322/© 2022 The Authors.

Published by Elsevier Masson SAS. This is an open access article under the CC BY-NC-ND license (<http://creativecommons.org/licenses/by-nc-nd/4.0/>).

1. Introduction

The outbreak of coronavirus disease 2019 (COVID-19), caused by severe acute respiratory syndrome coronavirus 2 (SARS-CoV-2), has led to a pandemic. Despite treatments and vaccines, this highly infectious disease continues to affect human health [1]. Vaccines are considered the most effective and economical means to prevent and control this pandemic [2]. However, the emergence of SARS-CoV-2 variants with spike (S) protein mutations that confer resistance to neutralization might threaten the global impact of mass vaccination campaigns. Due to altered virus-host cell interactions, emerging virus variants with enhanced transmissibility might rapidly spread around the world [3]. Therefore, there remains an urgent need for the development of additional treatments, such as affordable and accessible antiviral agents, to relieve the severity and mortality of COVID-19.

Traditional Chinese medicine (TCM) has played and continues to play an important role in the prevention and treatment of several viral pneumonias, including COVID-19 [4,5] and severe acute respiratory syndrome (SARS) in 2003 [6]. Some TCM prescriptions can not only inhibit viral replication directly but also attenuate excessive proinflammatory responses and tissue lesions caused by viruses [7]. Qingfei Paidu Decoction (QFPDD) has been commonly recommended for the treatment of COVID-19 by the General Office of National Health Commission and the Office of National Administration of Traditional Chinese Medicine of China [8]. In general, QFPDD is an optimized combination of four classic TCM recipes, each of which is widely used to treat diseases such as colds, fevers and flu in China [9,10]. Based on the theoretical system of TCM, physicians can combine and adjust the general prescriptions based on the symptoms of diagnosed patients to increase the curative effect and avoid potential adverse reactions [11,12]. Several retrospective multicentre cohort studies have demonstrated a satisfactory safety profile for QFPDD, and its early application is associated with favourable outcomes in patient recovery, viral shedding and course of the disease [13,14]. Studies based on network pharmacology have preliminarily clarified the active compounds of QFPDD in the treatment of COVID-19 [15]. However, the components of QFPDD and the targets of drug intervention for COVID-19 in these studies rely heavily on predictions and lack experimental validation, thus reducing the credibility of the results. Until now, the exact active components and mechanisms of QFPDD in the treatment of COVID-19 have not been elucidated based on modern pharmacological experiments, which undoubtedly hinders the rational application and quality control of this prescription and more seriously restricts its clinical application outside China. Recently, the serum-absorbed components of QFPDD were revealed by UHPLC-Q-Orbitrap HRMS assay [16], and these findings provide an important basis for in-depth research on the active components and mechanisms of QFPDD in the treatment of COVID-19.

Previous studies on TCM against COVID-19 have mainly focused on finding virus-targeted compounds, including virus entry inhibitors and key enzyme inhibitors of viral replication [17,18]. However, resistance to virus-targeted agents is a potential major obstacle to developing effective therapies due to mutations in SARS-CoV-2. Host-directed agents that act on the virus-host interactome potentially offer durable, broad-spectrum treatment modalities for viral infections [19]. For instance, transmembrane serine protease 2 (TMPRSS2) inhibitors were reported as potential treatments for COVID-19 because TMPRSS2 plays a key role in mediating viral entry [20,21].

Many studies have shed light on the SARS-CoV-2-host interactome at the cellular and host levels. For example, Blanco-Melo et al. analysed the gene expression profiles of multiple cell types after virus infection and showed that the overall transcriptional footprint of SARS-CoV-2 infection was distinct compared to that of other highly pathogenic coronaviruses and common respiratory viruses [22]. Lieberman et al. determined the gene expression of nasopharyngeal swabs from COVID-19 patients and presented the differential expression profile of host-specific genes after SARS-CoV-2 infection [23].

In this study, differentially expressed genes (DEGs) as a virus-host interactome for COVID-19 were obtained from SARS-CoV-2-infected cells by bioinformatics methods, and serum-absorbed components of QFPDD were analysed by systematic pharmacology. The antiviral and anti-inflammatory activities of QFPDD against clinically isolated SARS-CoV-2 in vitro were carried out to verify the predicted key results. Consequently, our results further reveal the effective components and underlying mechanisms of QFPDD, providing a scientific basis for QFPDD as a potential agent for clinical application in the prevention and treatment of COVID-19.

2. Materials and methods

2.1. Materials

Details of all compounds used in this study are shown in **Supplementary Table 1**. All compounds were dissolved separately in dimethyl sulfoxide (DMSO) at a stock concentration of 100 mM. Phorbol 12-myristate 13-acetate (PMA) was purchased from Topscience (Shanghai, China). Cell Counting Kit-8 (CCK-8) was purchased from Dojindo (Kumamoto, Japan). An ELISA kit for human interleukin-6 (IL-6) was purchased from Affymetrix (San Diego, CA, USA). ELISA kits for human interleukin-1 β (IL-1 β) and human C-X-C motif chemokine ligand 10 (CXCL-10) were purchased from BioLegend (San Diego, CA, USA).

2.2. Cell lines, virus and plasmids

The African green monkey kidney cell line (Vero-E6), human acute monocytic leukaemia cell line (THP-1), human ileocecal carcinoma cell line (HRT-18) and human embryonic kidney cell line 293 T (HEK-293 T) were purchased from American Type Culture Collection (Manassas, VA, USA). HEK-293 T cells stably expressing human ACE2 (ACE2-293 T) were established by our laboratory. Cells were maintained in Dulbecco's modified Eagle's medium (DMEM) or RPMI-1640 medium supplemented with 10% foetal bovine serum (FBS) and 1% penicillin-streptomycin in a humidified 5% CO₂ atmosphere at 37 °C. All reagents for cell culture were purchased from Gibco (Thermo Fisher, MA, USA). Human coronavirus OC43 (HCoV-OC43) was obtained from the State Key Laboratory of Respiratory Disease (Guangzhou Medical University, Guangdong, China).

The envelope-expressing plasmids SARS-CoV-2 S (*pcDNA3.1-SARS-CoV-2-S*, *pAAV-IRES-EGFP-SARS-CoV-2-S*) and SARS-CoV S (*pcDNA3.1-SARS-CoV-S*) were kindly provided by Dr. Shibo Jiang (Fudan University, Shanghai, China). Four envelope-expressing plasmids S protein variants of SARS-CoV-2, including D614G (substitution of aspartate (D) to glycine (G) at site 614 in S protein), E484K (substitution of glutamic acid (E) to lysine (K) at site 484 in S protein), N501Y (substitution of asparagine (N) to tyrosine (Y) at site 501 in S protein), P681H (substitution of proline (P) to histidine (H) at site 681 in S protein), and the luciferase reporter-expressing plasmid *pNL4-3*. *Luc.R⁻E⁻* were maintained in our laboratory. The plasmid *pAAV-IRES-EGFP* was purchased from Hedghog Bio (Shanghai, China).

2.3. Data retrieval and processing

The Gene Expression Omnibus (GEO) database (<http://www.ncbi.nlm.nih.gov/geo>) was used to search for a COVID-19-related gene expression microarray. First, the keywords "(COVID-19 OR SARS-CoV-2) AND GEO [entry type] AND \"Homo sapiens\"[porgn]" were used to search for the available data related to the subject, followed by the study type (expression profiling by array) to further screen out the candidate microarray datasets. Datasets with an experimental design that met the type of case-control study were selected.

2.4. Datasets analyses

The gene expression matrix and attached annotation document for each array dataset included in the final analysis were downloaded from the GEO database. The annotation document was used to annotate the gene name of the gene expression microarray. If multiple probes mapped to the same gene symbol, the mean expression value was adopted. Subsequently, the Limma package in R software was applied to identify DEGs between control samples and case samples in each gene expression microarray with the cut-off criteria $|\log_2\text{-fold change (FC)}| > 0.5$ and adjusted p value < 0.05 . Third, the Robust Rank Aggregation (RRA) R package was used to integrate all the ranked gene lists of datasets. The RRA method precludes the substantial heterogeneity and error of each experiment caused by different technological platforms or statistical methods. Theoretically, the smaller is the p value for the RRA results, the higher is the gene ranks and credibility of DEGs [24]. Genes with adjusted p values < 0.05 and $|\text{FC}| > 0.5$ were considered robust DEGs in the final gene list. Finally, the COVID-19 DEGs set was obtained by merging the DEGs from all the datasets included in the final analysis. In addition, according to the results of differential expression analysis in each dataset, a heatmap and volcano plot were constructed using R software.

2.5. Serum-absorbed compounds and corresponding targets of QFPDD

The list of serum-absorbed compounds in QFPDD were kindly provided by Dr. Guangbo Ge (Shanghai University of Traditional Chinese Medicine, Shanghai, China), who developed a method based on UHPLC-Q-Orbitrap HRMS to identify absorbed prototypes as well as the metabolites in mouse serum following oral administration of QFPDD [16]. Subsequently, the serum-absorbed compounds and their corresponding targets were collected from the Traditional Chinese Medicine System Pharmacology Database (TCMSP, <http://lsp.nwu.edu.cn/>). Because the TCMSP database only contains the official full name, the UniProt database (<https://www.uniprot.org>) was used to convert target names into standard gene symbols.

2.6. Construction of the compound-target-pathway-disease regulatory network

A Venn diagram was applied to intersect compound targets with disease targets to obtain common compound-disease targets. Subsequently, to better understand and visualize the molecular regulatory mechanism of QFPDD in the treatment of COVID-19, a visual network of “compound-target-pathway-disease” interactions was constructed by Cytoscape software. By analysing the topological features of the network, the key compounds and targets were identified according to the degree value of the nodes.

2.7. Functional enrichment analysis for targets in the network

Bioinformatic annotation of targets was performed by using the “clusterprofiler” package of R software. The results of Gene Ontology (GO) and Kyoto Encyclopedia of Genes and Genome (KEGG) enrichment analyses were used to decipher the potential molecular mechanisms of QFPDD in the treatment of COVID-19. Enrichment results with an adjusted p value < 0.05 were identified as statistically significant.

2.8. Cytotoxicity assay

The cytotoxicities of the test compounds on different target cells were analysed by CCK-8 assays. Briefly, ACE2-293 T, HRT-18 and Vero-E6 cells were seeded in a 96-well plate at 1×10^4 cells/well and allowed to adhere for 24 h. THP-1 cells were incubated with PMA (80 ng/mL) for 48 h, which was then exchanged with fresh medium for 24 h. The cells were treated with a serial dilution of compounds for 48 h. CCK-8

solution was added, the cells were incubated at 37 °C for 2 h, and the optical density (OD) at 450 nm was then measured using a microplate reader. The half-maximal cytotoxic concentration (CC₅₀) was calculated using GraphPad Prism 8 software (GraphPad Software, CA, USA). Follow-up experiments were carried out under the condition that all compounds had no significant toxicity towards cells.

2.9. Pseudotyped virus infection assays

The infectivity of pseudotyped SARS-CoV-2 S and SARS-CoV S in target cells was determined by a single-cycle infection assay as described previously [25]. Briefly, pseudovirus (PsV) was produced by cotransfection of HEK-293 T cells with a backbone plasmid (*pNL43. Luc. RE*) and plasmids encoding either SARS-CoV-2 S or SARS-CoV S by using PolyJet transfection reagent (SignaGen, MD, USA). Target cells (ACE2-293 T and Vero-E6) were seeded into 96-well plates at a density of 1×10^4 cells per well and incubated for 24 h. A mixture consisting of gradient concentrations of compounds and an equal volume of pseudovirus was added to each well. After 48 h, the cells were lysed, and luciferase activities were quantified by a luciferase assay system (Promega, Madison, WI, USA). Chloroquine (CQ) was used as a positive control. The half-maximal inhibitory concentration (IC₅₀) was calculated as the final concentration of compounds that caused a 50% reduction in relative luminescence units compared to the level of the virus control subtracted from that of the cell control. The IC₅₀ values are expressed as the means \pm SDs from independent experiments and were calculated using GraphPad Prism 8 software.

2.10. Cell-cell fusion assay

The SARS-CoV-2 S protein-mediated cell-cell fusion assay was performed as described previously [25]. Briefly, HEK-293 T cells were transfected with the vehicle plasmid *pAAV-IRES-GFP* or *pAAV-IRES-GFP-SARS-CoV-2 S* by using PolyJet to construct effector cells. Vero-E6 cells were incubated in 96-well plates at a density of 1×10^4 cells per well for 6 h followed by the addition of effector cells with or without compounds. After 6 h, three random fields in each well were imaged by inverted fluorescence microscopy (Zeiss, Jena, Germany). The percent inhibition of cell-cell fusion was calculated using the formula described previously [25].

2.11. ELISA for cytokines

The levels of the cytokines IL-6, IL-1 β and CXCL-10 were measured by ELISA using capture and detection antibodies. For monocyte to macrophage differentiation, THP-1 cells were incubated with PMA (80 ng/mL) for 48 h in 96-well plates at a concentration of 3×10^4 cells/well and changed with fresh medium for 24 h. The cells were treated with SARS-CoV-2 S PsV for 24 h after incubation with the test compounds for 12 h. The cell culture supernatants were collected and analysed according to the manufacturer's instructions; OD at 450 nm was measured by a microplate reader (BioTek, Vermont, USA).

2.12. Live SARS-CoV-2 infection assay

Live SARS-CoV-2 (isolate Wuhan-Hu-1) inhibition assays were performed by the Wuhan Institute of Virology, Chinese Academy of Sciences, as described [26]. All infection experiments were performed in a biosafety level-3 laboratory. Briefly, Vero-E6 cells were pretreated with the test compounds for 1 h and then infected with SARS-CoV-2 (MOI = 0.001) for 1 h. Subsequently, fresh medium with the test compounds was added, and viral total RNA in the supernatants was extracted using a MiniBEST Viral RNA/DNA Extraction Kit (Takara, Tokyo, Japan) after 24 h of incubation. S gene copies were quantified from viral cDNA by a standard curve using an ABI 7500 (Takara TB Green Premix Ex Taq II, Tokyo, Japan) after reverse transcription. DMSO and CQ were used as

negative and positive controls, respectively. IC₅₀ values are expressed as the mean ± SD from independent experiments and calculated using GraphPad Prism 8 software.

2.13. Indirect immunofluorescence assay

The protective effects of the test compounds on Vero-E6 cells infected with SARS-CoV-2 were examined by observing the virus distribution profile reflected by viral nucleoprotein (NP) expression. Briefly, Vero-E6 cells from the live SARS-CoV-2 infection assay were fixed with 4% paraformaldehyde and then permeabilized with 0.2% Triton X-100 (Sigma, MO, USA) [26]. After blocking nonspecific binding sites with 2% skim milk, the cells were incubated with polyclonal rabbit anti-NP antibodies and a secondary goat anti-rabbit IgG H&L (Alexa Fluor® 488) (Abcam, Cambridge, UK). DAPI was used for nuclear staining, and fluorescence images were acquired by an inverted fluorescence microscope (Zeiss, Jena, Germany).

2.14. Molecular docking

Molecular docking was performed using the Sybyl-8.1 surflex-dock module (Tripos, Inc. St. Louis, MO, USA). Here, the structure of ACE2 protein was downloaded from the Protein Data Bank (PDB: 6acg). Shedding of small-molecule ligands and water of ACE2 protein and other necessary modifications were applied to produce a simulated physiological environment [27]. To generate the ProtoMol, a threshold parameter of 0.5 and a bloat parameter of 0 Å were set. The generated ProtoMol is a computational representation of a ligand with the potential interaction with the binding site, and Kollman all-charges were added. Staged minimization with 2000 steps at each stage and the GeoMx model were then chosen for molecular preparation. Sequentially, OA was docked into the binding sites of ACE2 protein. The minimum RMSD between final poses and other parameters were set to 0.5 Å to distinguish conformations from the default.

2.15. HCoV-OC43 infection assay

HCoV-OC43 was grown and propagated in HRT-18 cells cultured with RPMI-1640 and 2% FBS. For compound treatment studies, HRT-18 cells were seeded into 12-well plates at a density of 4×10^5 cells per well and incubated for 24 h. The cells were pretreated with serial dilutions of compounds at the indicated concentrations for 1 h prior to HCoV-OC43 infection at an MOI of 0.05. Samples were collected after cells were treated with a mixture of compounds and viruses for 24 h. Total RNA in the adherent cells was extracted using a Cell Total RNA Isolation Kit (FOREGENE, Chengdu, China) according to the manufacturer's instructions. Real-time PCR (RT-PCR) was accomplished using a Light-Cycler 480 sequence detector system (Roche, Mannheim, Germany) with SYBR® Premix Ex Taq™ II reagents (Takara, Tokyo, Japan) according to the manufacturer's instructions. The primers used for the HCoV-OC43 nucleoprotein (NP) gene, HCoV-OC43 spike protein (SP) gene and human GAPDH gene are as follows:

HCoV-OC43 NP-sense: 5'-AGCAACCAGGCTGATGTCAATACC-3'.

HCoV-OC43 NP-antisense: 5'-AGCAGACCTTCTGAGCCTTCAAT-3'.

HCoV-OC43 SP-sense: 5'-GCCAACTCTTCGAACAGC-3'.

HCoV-OC43 SP-antisense: 5'-TGGGTTGCAGCTGTCTGTGA-3'.

GAPDH-sense: 5'-AGGGCAATGCCAGCCCCAGCG-3'.

GAPDH-antisense: 5'-AGGCGTCGGAGGGCCCCCTC-3'.

Gene expression was analysed using quantitative RT-PCR with GAPDH as an internal control. The IC₅₀ values were calculated by HCoV-OC43 NP gene expression. The expression of HCoV-OC43 NP was detected by indirect immunofluorescence assay and western blot assay with primary antibody 40643-T62 (Sinobiological, Beijing, China) and secondary goat anti-rabbit IgG H&L (YF®594) (Bioscience, Shanghai, China) following the routine experimental procedure described above and in the previous study [28].

2.16. Statistical analysis

The data are presented as the means ± standard deviations and were analysed using SPSS software, v22.0 (IBM, NY, USA). Student's t test or ANOVA was applied as appropriate. Outliers were excluded using Grubb's method. A *p* value of < 0.05 was considered statistically significant, and the probability level is indicated by single asterisks or multiple asterisks (*) (* *p* < 0.05 and ** *p* < 0.01).

3. Results

3.1. Differentially expressed genes in SARS-CoV-2-infected individuals

According to the above criteria, the GSE147507 and GSE152075 datasets were used in this study. The GSE147507 dataset contains two subdatasets: A549-ACE2 cells, a type of transformed lung alveolar cell (A549) transduced with a vector expressing human ACE2, and transformed lung-derived Calu-3 cells. Both were mock-infected with SARS-CoV-2. The GSE152075 dataset contains RNA-sequencing profiles of nasopharyngeal swabs from 430 SARS-CoV-2-infected individuals and 54 negative controls, including host gene expression, viral load, age, and sex across infection status.

The microarray datasets were standardized to remove individual differences between samples. The results showed that the homogeneity of the data met the requirements (**Supplementary Fig. 1**). Subsequently, DEGs were identified in each dataset by using R software according to the cut-off criteria. A total of 2657 DEGs were identified by merging three microarray subdatasets and deleting duplicates (**Supplementary Table 2**). The volcano plots of the three microarrays are shown in **Fig. 1A-C**. The overall results from the RRA analysis are presented in **Supplementary Table 3**. The heatmap of the top 20 up- and down-regulated DEGs is shown in **Fig. 1D**.

3.2. Compound-target-pathway-disease regulatory network

A total of 195 compounds (104 prototypes and 91 metabolites) were identified in mouse serum after oral administration of QFPDD, and prototype compounds were further explored in this study. A total of 70 compounds and 313 corresponding targets were identified in the TCMSP database after deleting untargeted compounds and duplicate targets (**Supplementary Table 4**).

To reveal the key targets of QFPDD, the intersection of targets of absorbed compounds in serum and DEGs of SARS-CoV-2-infected individuals were identified by a Venn diagram. A primary compound-target-pathway-disease regulatory network was constructed, including 54 biologically active compounds, 66 targets and the top 10 KEGG pathways (**Fig. 2**). All intersecting targets and their corresponding compounds are listed in **Supplementary Table 5**. Through network topological feature analysis, 10 high-degree compounds were identified in **Table 1**, including resveratrol (RE), wogonin (WO), daidzein (DA), luteolin (LU), oroxylin A (OA), hesperetin (HE), isoliquiritigenin (IS), naringenin (NA), scutellarin (SC), and tectorigenin (TE). These ten compounds regulated most of the DEGs of SARS-CoV-2-infected individuals and might be the key active compounds of QFPDD in the treatment of COVID-19.

3.3. Functional enrichment analysis of common targets

The results of functional enrichment showed that 66 drug-disease common targets were significantly enriched in 122 KEGG pathways and 50 GO terms according to the cut-off criterion of adjusted *p* value < 0.05 (**Supplementary Table 6**). As presented in **Fig. 3A**, the top 20 most significant KEGG pathways were mainly enriched in inflammation- and infection-related signalling pathways, such as the NF-kappa B signalling pathway, Toll-like receptor signalling pathway, Epstein-Barr virus and influenza A infection signalling pathway. The top 20 most

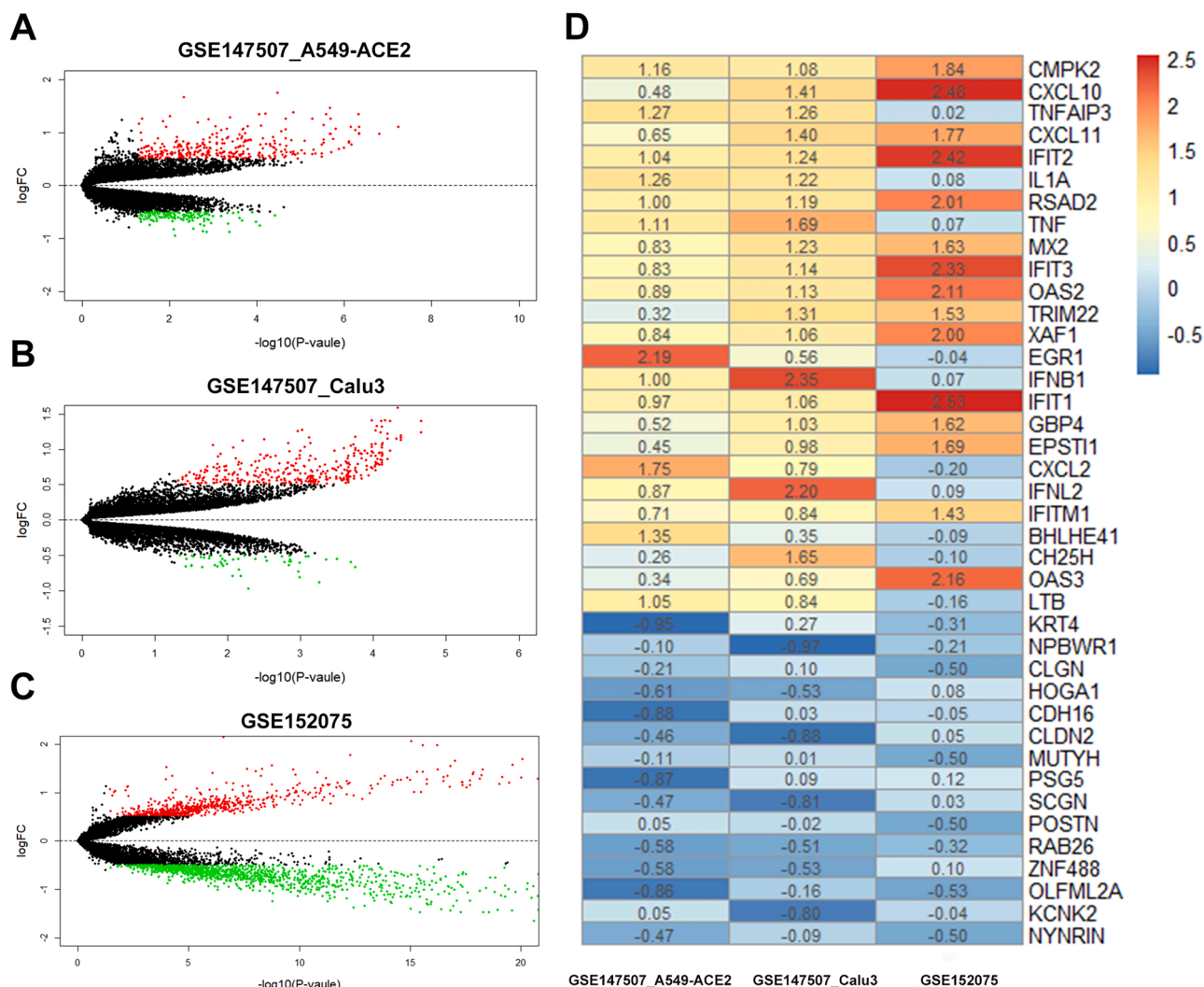


Fig. 1. Differentially expressed genes in SARS-CoV-2-infected individuals. (A-C) Volcano plots. The red points represent upregulated genes, and the green points represent downregulated genes. The black points indicate genes with no significant difference. (D) Heatmap. Adjusted p value < 0.05 & $|FC|$ > 0.5 were used.

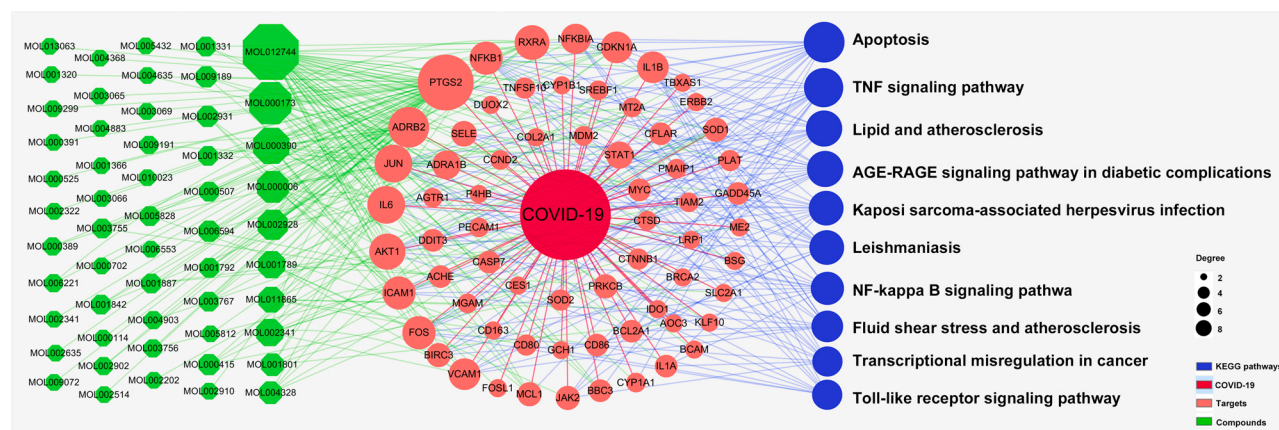


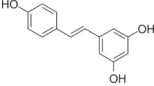
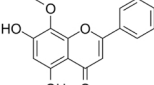
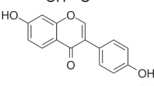
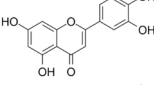
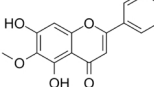
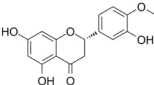
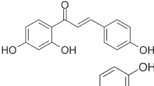
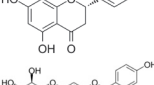
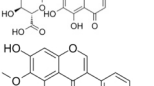
Fig. 2. Compound-target-pathway-disease regulatory network of QFPDD in the treatment of COVID-19. This network contained 66 genes, 54 compounds, and the top 10 significant KEGG pathways. The element size represents the degree value.

significant GO terms included the response to cytokine receptor binding, virus receptor activity and activated transcription factor binding (Fig. 3B).

3.4. OA, HE and SC effectively inhibit infection by live SARS-CoV-2

The 10 high-degree predicted compounds obtained after the screening of the compound-target-pathway-disease interaction network

Table 1
Information on the 10 high-degree compounds.

Molecule Name	Chemical structure	TCMSP MOI ID	Pubchem CID	Degree
Resveratrol		MOL012744	445154	42
Wogonin		MOL000173	5281703	18
Daidzein		MOL000390	5281708	14
Luteolin		MOL000006	5280445	11
Oroxylin A		MOL002928	5320315	10
Hesperetin		MOL002341	72281	8
Isoliquiritigenin		MOL001789	638278	8
Naringenin		MOL004328	439246	5
Scutellarin		MOL002931	185617	4
Tectorigenin		MOL003767	5281811	3

further validated the antiviral activities against infection by live SARS-CoV-2 in vitro. Vero E6 cells were infected with 100 TCID₅₀ of live virus and incubated with compounds at different dilution concentrations for 24 h. As shown in Table 2, three compounds, OA, HE and SC, significantly inhibited SARS-CoV-2 replication in Vero-E6 cells, with IC₅₀ values of 31.39 ± 0.07, 49.99 ± 0.66 and 22.47 ± 0.19 μM, respectively. In addition, the inhibition of SARS-CoV-2 infection by TE at concentrations up to 100 μM was approximately 48.31% (data not presented). NP, a multifunctional RNA-binding protein for viral RNA transcription and replication, is highly expressed during SARS-CoV-2 infection [29]. We further analysed the effects of these compounds on viral NP expression by indirect immunofluorescence analysis. Consistently, all three compounds significantly inhibited the expression of NP in Vero-E6 cells in a dose-dependent manner (Fig. 4A). Chloroquine (CQ) at 10 μM was used as a positive control. Moreover, OA, HE and SC showed minimal levels of cellular toxicity in Vero-E6 cells, with CC₅₀ values of more than 200 μM (Fig. 4B-D and Table 2). These results indicated that OA, HE and SC may be the major active compounds of QFPDD against SARS-CoV-2 infection.

3.5. OA inhibits the entry of SARS-CoV-2 PsV into target cells

The surrogate PsV system has become an ideal tool for identifying antiviral agents and studying the entry of SARS-CoV-2 without safety concerns [30,31]. Our previous studies showed that some compounds exhibited potent antiviral activity against the entry of SARS-CoV-2 PsV into target cells [26]. Thus, we further detected the inhibitory activity of 10 high-degree compounds against the entry of SARS-CoV-2 S PsV using the surrogate PsV system. The results showed that of the ten compounds,

only OA exhibited significant inhibitory activity against SARS-CoV-2 S PsV infection in both ACE2-293 T cells and Vero-E6 cells in a dose-dependent manner, with IC₅₀ values of 15.03 ± 1.46 and 15.08 ± 2.19 μM, respectively (Fig. 5A, B). To investigate whether OA has a similar effect on SARS-CoV infection, which is closely related to SARS-CoV-2 infection and employs ACE2 for cell entry, we conducted a pilot experimental test in vitro on anti-SARS-CoV S PsV activity. We found that OA exhibited similar inhibitory activity against the entry of SARS-CoV S PsV into 293 T-ACE2 cells (Fig. 5A, B).

Compared to the wild-type S protein of SARS-CoV-2, its variants showed stronger binding activities to ACE2 receptors, thereby increasing virus transmission efficiency in host cells [32]. Accordingly, we further tested the potential inhibition of OA on the entry of four S protein variants PsV (D614G, N501Y, E484K and P681H) of SARS-CoV-2. The results showed that OA had significant inhibitory activities on the entry of four S protein variants, PsV, into ACE2-293 T cells in a dose-dependent manner, with IC₅₀ values of 18.11 ± 0.67, 13.62 ± 1.24, 18.98 ± 3.20 and 19.56 ± 2.39 μM, respectively (Fig. 5C). CQ was used as a positive control (Fig. 5D). In addition, the cytotoxicity assay showed that OA had no or only slight cytotoxicity towards both ACE2-293 T and Vero-E6 cells at concentrations up to 80 μM.

3.6. OA inhibits SARS-CoV-2 S protein-mediated cell-cell fusion

The S protein of SARS-CoV-2 binds to the ACE2 receptor to facilitate fusion and eventually enter the target cells. To further confirm the possible mechanism of OA, we determined the effect of OA on SARS-CoV-2 S protein-mediated cell-cell fusion as described previously [25]. As shown in Fig. 6A, OA significantly inhibited the S-mediated 293 T/SARS-CoV-2/EGFP and Vero E6 cell-cell fusion, resulting in a reduction in syncytium formation in a dose-dependent manner.

Polymerization of heptad repeat 1 (HR1) and heptad repeat 2 (HR2) in the S2 subunit of the S protein to form the six-helical bundle (6-HB) is the key process of SARS-CoV-2-mediated membrane fusion [33]. Our previous study found that salvianolic acid C inhibits SARS-CoV-2-mediated membrane fusion by interfering with the formation of 6-HB [34]. However, further analysis showed that OA inhibited cell-cell fusion mediated by the SARS-CoV-2 S protein independent of interfering with the formation of 6-HB (Fig. 6B).

Molecular docking has become an important technique for studying the interaction between the ligand and receptor [35]. Accordingly, molecular docking studies were performed to explore whether OA has the ability to bind the ACE2 protein. We used the X-ray structure (PDB: 6acg) of the SARS-CoV-2 RBD/ACE2-B0AT1 complex as the docking protein [36]. Using Sybyl-8.1 software, OA was docked with the pre-treated 6acg protein. OA binds to the collectrin-like domain cavity of ACE2 protein, as shown in Fig. 6C. The 4-carbon oxygen atom and 5-hydroxyl oxygen atom of the flavone body form hydrogen bonds with LYS416. The 5-hydroxy hydrogen atom of the flavone body forms hydrogen bonds with GLU536 and LYS541. The oxygen atom of the 6-methoxy group of the flavone body forms a hydrogen bond with HIS535, as shown in Fig. 6D. Therefore, OA can perfectly bind with ACE2, which may be one of the mechanisms by which OA inhibits SARS-CoV-2 entry.

3.7. Inhibitory effects of active compounds on viral-induced cytokine release

The S protein of SARS-CoV-2 triggers potent inflammatory responses in macrophages and epithelial cells [37], and the inhibitory effects of QFPDD on inflammation caused by SARS-CoV-2 have been confirmed by a large number of studies [8]. Therefore, we analysed the effective compounds and mechanisms of the anti-inflammatory effect of QFPDD. As shown in Fig. 7A, the 10 high-degree compounds in Table 1 regulated the NF-kappa B signalling pathway, the Toll-like receptor signalling

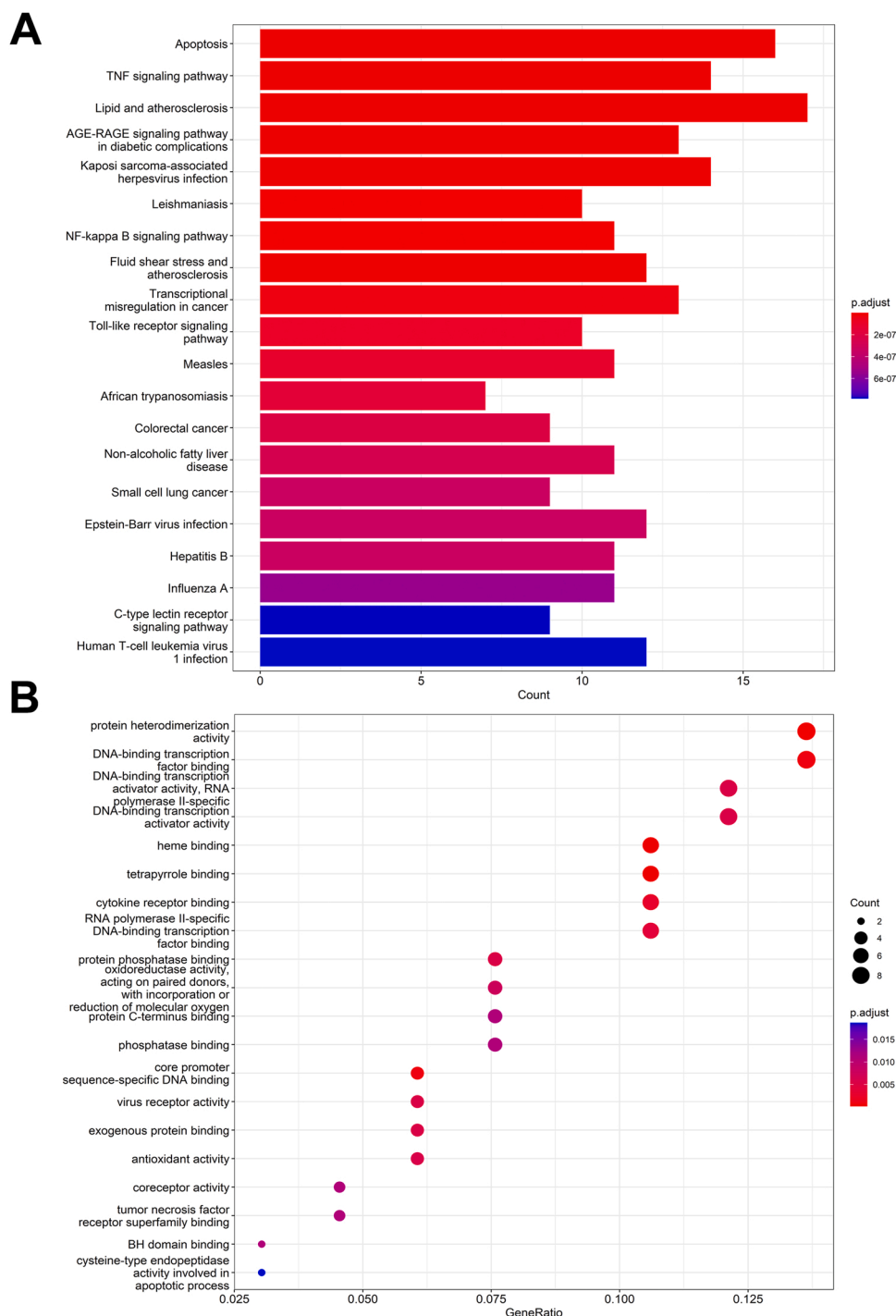


Fig. 3. Functional enrichment analysis for identification of the targets of QFPDD on COVID-19. (A) Top 20 most significant KEGG pathways. (B) Top 20 most significant GO terms. The cut-off criterion was an adjusted *p value* < 0.05.

Table 2
Anti-SARS-CoV-2 activities and cytotoxicities of three compounds in Vero-E6 cells in vitro.

Compounds	IC ₅₀ (μM)	CC ₅₀ (μM)	SI
Oroxylin A (OA)	31.39 ± 0.07	> 200.00	> 6.37
Hesperetin (HE)	49.99 ± 0.66	> 200.00	> 4.00
Scutellarin (SC)	22.47 ± 0.19	> 200.00	> 8.90

IC50: half-maximal inhibitory concentration.

CC₅₀: half-cytotoxic concentration.

SI: selectivity index as CC₅₀/IC₅₀

pathway, and the TNF signalling pathway, which have been reported to be closely related to SARS-CoV-2-induced inflammatory responses [38, 39]. Moreover, the anti-inflammatory effects of these 10 compounds have been widely confirmed in several studies [40,41]. Herein, we further investigated the effects of these compounds on cytokine expression in THP-1 macrophages challenged with the SARS-CoV-2 S protein. As shown in Fig. 7B and Supplementary Fig. 2 A, ten tested compounds at different concentrations except SC significantly decreased the release of IL-6 from THP-1 cells. Furthermore, OA, TE and IS at different concentrations inhibited the release of both CXCL-10 and IL-1β (Fig. 7C, D and Supplementary Fig. 2B, C), NA and LU at different

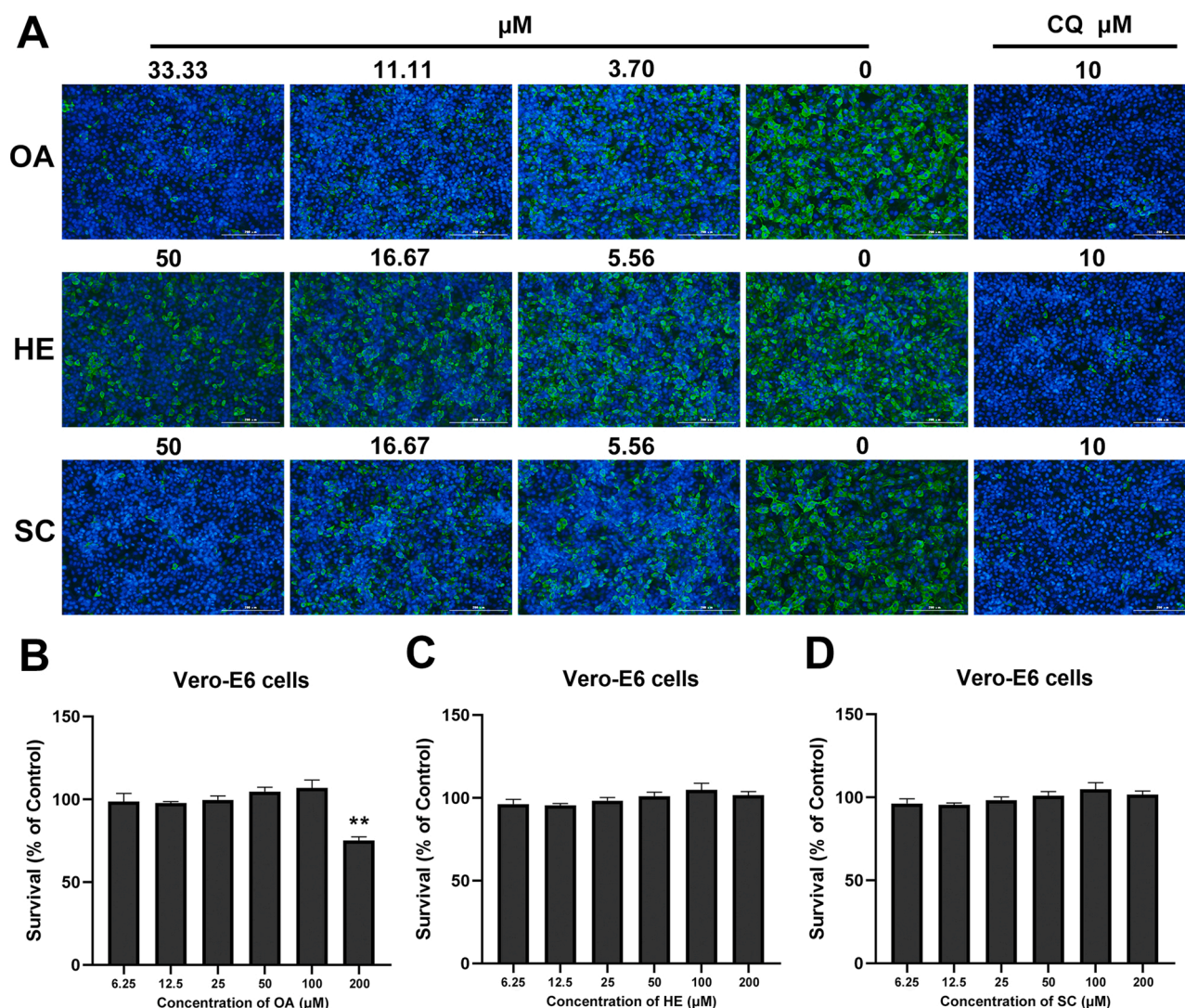


Fig. 4. Inhibitory activity of compounds on live SARS-CoV-2 infection in vitro. (A) SARS-CoV-2 NP expression (green) was detected by indirect immunofluorescence assay. Nuclei (blue) were stained with DAPI, scale bar = 200 μm. CQ was used as a positive control. The cytotoxicities of OA (B), HE (C) and SC (D) towards Vero-E6 cells were determined by CCK-8 assays. The data are presented as the means ± SDs of triplicate samples from a representative experiment (* $p < 0.05$, ** $p < 0.01$).

concentrations inhibited the release of CXCL-10 (Fig. 7C), and RE at different concentrations inhibited the release of IL-1β (Fig. 7D and Supplementary Fig. 2 C).

3.8. OA, HE and SC effectively inhibit infection by live HCoV-OC43

To investigate whether OA, HE, and SC have inhibitory effects on other types of coronaviruses, we tested their inhibitory effects on HCoV-OC43, which is considered to be the most common human coronavirus worldwide and is typically associated with mild respiratory tract infections [42]. HRT-18 cells were infected with 100 TCID₅₀ of live HCoV-OC43 and incubated with compounds at different dilution concentrations for 24 h. As shown in Fig. 8D-E, OA, HE and SC significantly inhibited the expression of HCoV-OC43 NP and SP genes in HRT-18 cells, with IC₅₀ values of 18.68 ± 0.06 , 31.46 ± 0.27 and 63.27 ± 0.50 μM, respectively. Western blotting results showed that all three compounds inhibited the expression of HCoV-OC43 NP protein, with OA and HE being more effective (Fig. 8F). We further analysed the effects of OA and HE on the expression of HCoV-OC43 NP protein by indirect immunofluorescence assay. The results showed that both could significantly inhibit the expression of the HCoV-OC43 NP protein in HRT-18

cells (Fig. 8G). Moreover, all three compounds showed minimal levels of cellular toxicity on HRT-18 cells, with CC₅₀ values of more than 400 μM (Fig. 8A-C). These results suggest that OA, HE and SC may be the main active compounds of QFPDD against common coronavirus infection.

4. Discussion

TCM prescriptions are widely used in the treatment of COVID-19 in China and have been proven to significantly alleviate the symptoms of the disease, delay the progression of mild disease to severe disease, improve cure rates and reduce mortality rates [11]. QFPDD is the only general prescription that has been for the treatment of COVID-19 patients, including patients with mild, moderate, and severe disease and critically ill patients. A comprehensive understanding according to the actual situation of the patients, particularly considering the age, physique, disease status, treatment process, medication effect, and underlying diseases, is necessary to make dialectical differentiations of the syndrome, disease, and treatment based on a traditional Chinese physician's clinical experience [43]. For clinical application, QFPDD is taken as a water decoction once a day and separately administered in the

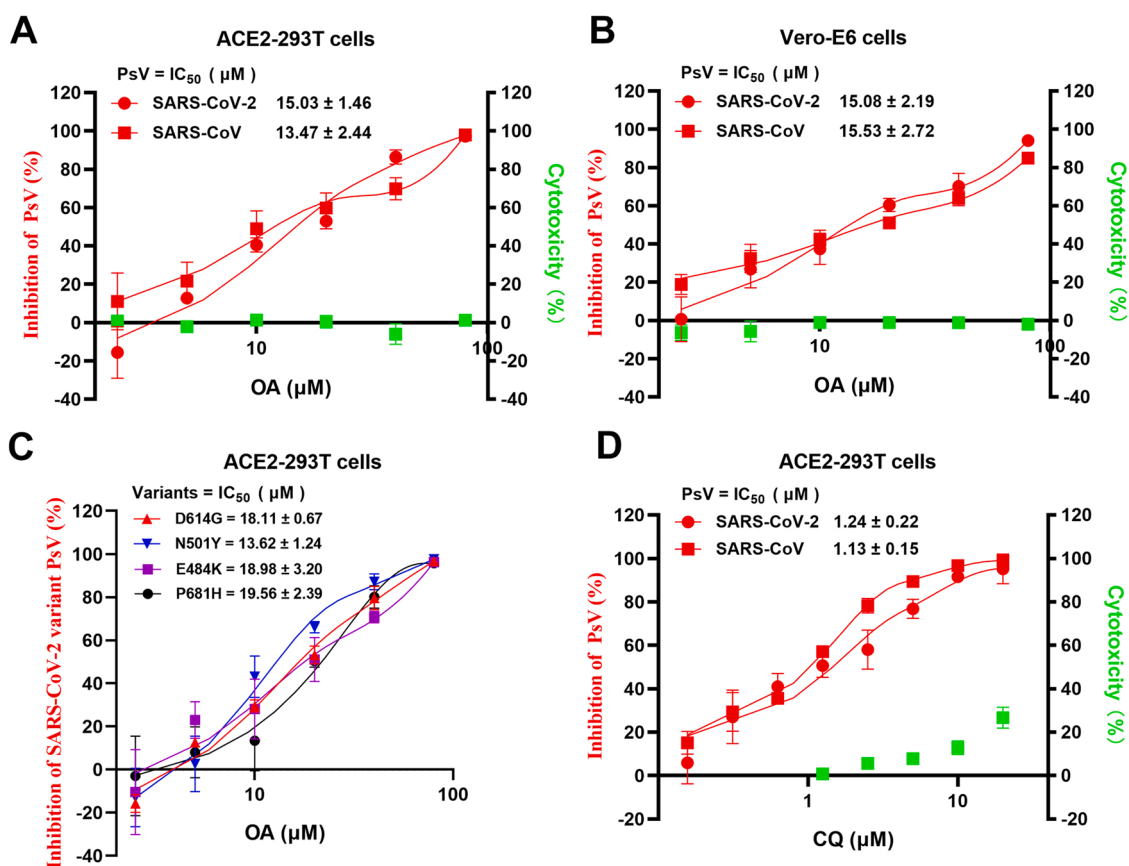


Fig. 5. OA inhibits the entry of SARS-CoV-2 PsV and SARS-CoV PsV into target cells. Inhibitory activity of OA against SARS-CoV-2 S PsV and SARS-CoV S PsV infection in ACE2-293 T (A) or Vero-E6 (B) cells. (C) Antiviral activity of OA against SARS-CoV-2 S variant PsV infection in ACE2-293 T cells. (D) Antiviral activity of CQ against SARS-CoV-2 S PsV and SARS-CoV S PsV infection in ACE2-293 T cells. The data are presented as the means ± SDs of triplicate samples from a representative experiment.

morning and at night 40 min after meals, resulting in a total of three doses during the course of treatment. If possible, half a bowl of rice water can be consumed after each time the decoction is administered, and those with body fluid deficiency can consume one bowl of rice water [12]. Although QFPDD has been proven to be a safe and effective prescription for the treatment of COVID-19, its active components and mechanisms remain unclear, particularly with respect to components affecting the virus-host interactome.

In this study, we constructed a compound-target-pathway-disease interaction network of QFPDD for the treatment of COVID-19 by targeting the virus-host interactome based on the absorbed components of QFPDD in mouse serum. Through network topological feature analysis, 10 high-degree compounds were predicted to be potentially associated with the clinical therapeutic effects of QFPDD against COVID-19. According to antiviral analysis in vitro, OA, HE and SC effectively suppressed infection by live SARS-CoV-2 in Vero-E6 cells and HCoV-OC43 in HRT-18 cells. Among them, OA is an O-methylated flavone found in *Scutellaria baicalensis*, which is reported to have various biological functions, including antiviral, anti-inflammatory, and anticancer activities [44]. The inhibitory effects of OA on enterovirus, influenza A virus and respiratory syncytial virus have been demonstrated in previous studies [45–47]. Most recently, Gao et al. showed that OA could inhibit the entry of SARS-CoV-2 S PsV into ACE2-293 T cells by binding to the ACE2 receptor, which is consistent with our molecular docking results [48]. Our research also confirmed that OA inhibited the entry of SARS-CoV-2 S PsV into target cells and inhibited SARS-CoV-2 S protein-mediated cell-cell fusion. Interestingly, OA also showed a significant inhibitory effect on HCoV-OC43, which enters cells via 9-O-acetylated sialic acid-mediated endocytosis [49], suggesting that

OA may exert its inhibitory effect on coronaviruses through a variety of mechanisms. It is worth noting that only oroxyloside, the glycoside form of OA, was identified as an active component in the water extract of QFPDD [5]. In general, oroxyloside needs to be hydrolysed to OA by intestinal enzymes for intestinal absorption [50]. This indicates that it might be a scientific and effective way to ascertain the active components of TCM by analysing the serum absorbed components in the prescription. SARS-CoV-2 hijacks and exploits autophagy to promote viral replication [51,52], and autophagy modulators have been verified to have anti-SARS-CoV-2 activity [20,53]. OA, a moderate inhibitor of cyclin-dependent kinase 9, blocks autophagy initiation by inactivating the SIRT1-FOXO3-BNIP3 axis and PINK1-PRKN pathway [54]. Whether the inhibition of SARS-CoV-2 infection by OA is also related to the regulation of autophagy needs further study.

HE is the aglycon of hesperidin. Both HE and hesperidin have been shown to inhibit SARS-CoV-2 S PsV infection by blocking the interaction between the S protein and ACE2 receptor and reducing ACE2 and TMPRSS2 expression [55,56]. HE has also been predicted using computational approaches to be a potent inhibitor of the main protease of SARS-CoV-2 [57]. Moreover, hesperidin was previously found to be effective against live SARS-CoV-2 infection in high-throughput screening experiments [58]. Our study further demonstrated that HE also significantly inhibited live SARS-CoV-2 and HCoV-OC43 infection in vitro. SC, as the major component of both breviscapine tablets and injections, has long been used in the treatment of cardiovascular disease owing to its ability to improve the cerebral blood supply [59,60]. Previous studies have shown that SC has antiviral activity against porcine reproductive and respiratory syndrome virus and human immunodeficiency virus in vitro [61,62]. Nevertheless, SC inhibits neither the entry

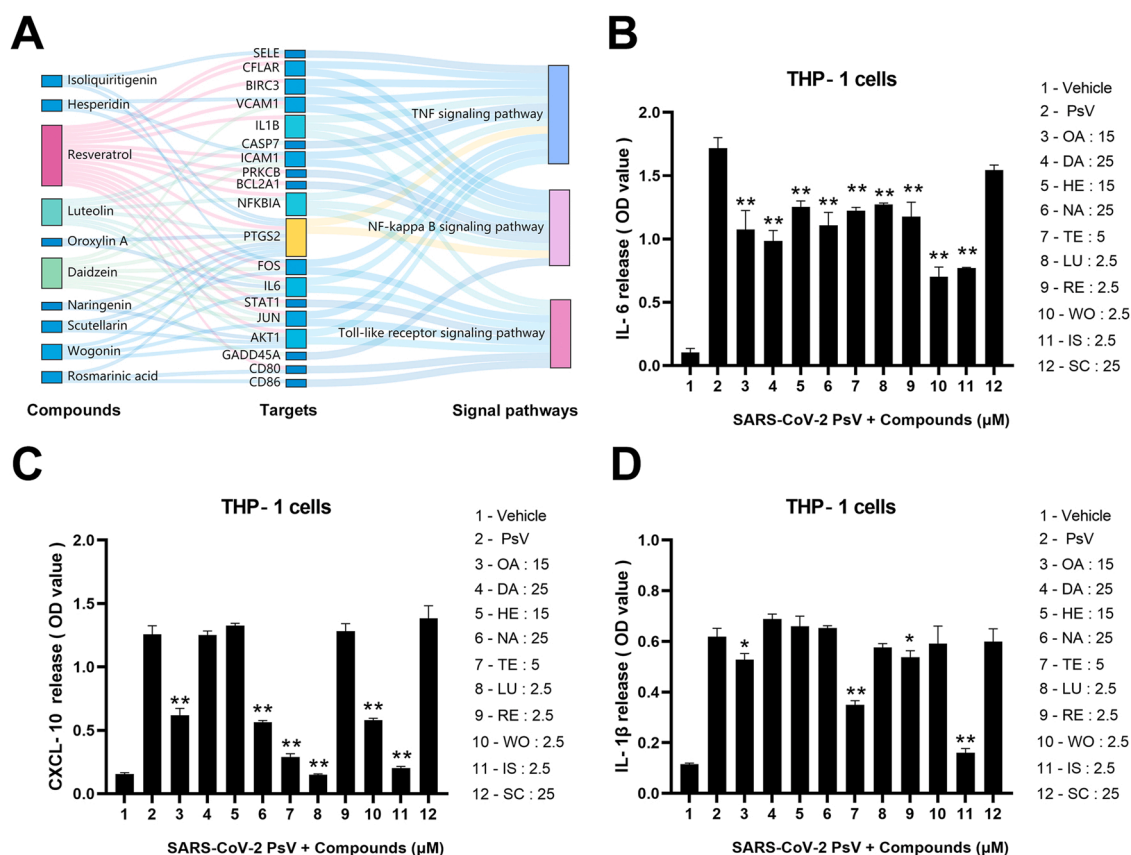


Fig. 7. The anti-inflammatory effect of QFPDD might be related to the effects of 10 high-degree compounds. (A) Inflammation-related signalling pathways regulated by 10 high-degree compounds. Effects of 10 high-degree compounds on IL-6 (B), CXCL-10 (C) and IL-1 β (D) release from SARS-CoV-2 S protein-challenged THP-1 cells. The data are presented as the means \pm SDs of triplicate samples from a representative experiment (* $p < 0.05$, ** $p < 0.01$, versus SARS-CoV-2 S protein).

syndrome in COVID-19, IL-6 is particularly important in the persistence of the proinflammatory milieu, and IL-1 β , CXCL-10, IL-2, IL-7 and IL-10 are critical for escalating disease complications [67,68]. Our results showed that the active components of QFPDD significantly inhibited the release of IL-6, IL-1 β and CXCL-10 from THP-1 macrophages challenged with SARS-CoV-2 S protein, which suggested that the anti-inflammatory effects of QFPDD may be attributed to the effects of these active components.

Several classic TCM recipes (e.g., Ma Xing Shi Gan decoction [69], She Gan Ma Huang decoction [70] and Xiao Chai Hu [71]) that comprise QFPDD have been widely used in the treatment of respiratory diseases for thousands of years in China [72]. TCM recipes with multicomponent, multitarget, and multimechanism characteristics potentially offer durable, broad-spectrum treatment modalities for viral infections. Interestingly, the aglycone or glycoside forms of OA, HE or SC have been elucidated as components of several TCM formulations, such as Shuanghuanglian preparation [64], Reduning injection [73], Jinzhen granule [74], Yinqiao powder [75] and Lianhuaqingwen capsule [76]. Similar to QFPDD, these formulations have also been recommended as effective therapeutic formulations against COVID-19 in China. These studies support that the three components might be the key active compounds of QFPDD in the treatment of COVID-19.

5. Conclusion

In this study, we applied an approach targeting the virus-host interactome to construct a compound-target-pathway-disease interaction network and clarify the active components and mechanisms of QFPDD in the treatment of COVID-19. By systematic pharmacology and antiviral in vitro analysis, we found that three components of QFPDD,

OA, HE and SC, exhibit potent antiviral activity against live SARS-CoV-2 virus and HCoV-OC43. Furthermore, we confirmed that the active components of QFPDD could clearly inhibit the release of IL-6, IL-1 β and CXCL-10 from THP-1 macrophages challenged with the SARS-CoV-2 S protein. This study provides an effective analysis method for in-depth study of the mechanisms of TCM prevention and treatment of diseases. Due to the complexity of the serum-absorbed compounds of QFPDD, more studies are needed to elucidate the interactions between the active components and their efficacies in vivo.

Funding

This study was supported by the National Natural Science Foundation of China (82273976 to L.L., 82073896 to L.L. and 82072276 to S. T.), Natural Science Foundation of Guangdong Province (2018B030312010 to L.L.), Guangdong Basic and Applied Basic Research Foundation (2019A1515010061 and 2021A1515011096 to L. L.), Construction Project of Influenza Prevention and Treatment Technology System of Chinese Medicine organized by Chinese Academy of Traditional Chinese Medicine (ZZ13-035-02 to L.L.), Guangzhou Science and Technology Basic and Applied Basic Research Foundation (202102080108 to L.L.), and China Postdoctoral Science Foundation (2020M681947 to J.Q.).

CRediT authorship contribution statement

Yuyun Li: Methodology, Investigation, Experimental, Writing – original draft. **Yan Wu, Siyan Li, Xin Zhang, Daohua Xu, Zeren Shou:** Investigation, Experimental, Writing – original draft. **Jiayin Qiu, Suiyi Tan, Shuyin Gu, Chenliang Zhou, Yibin Li:** Investigation, Validation,

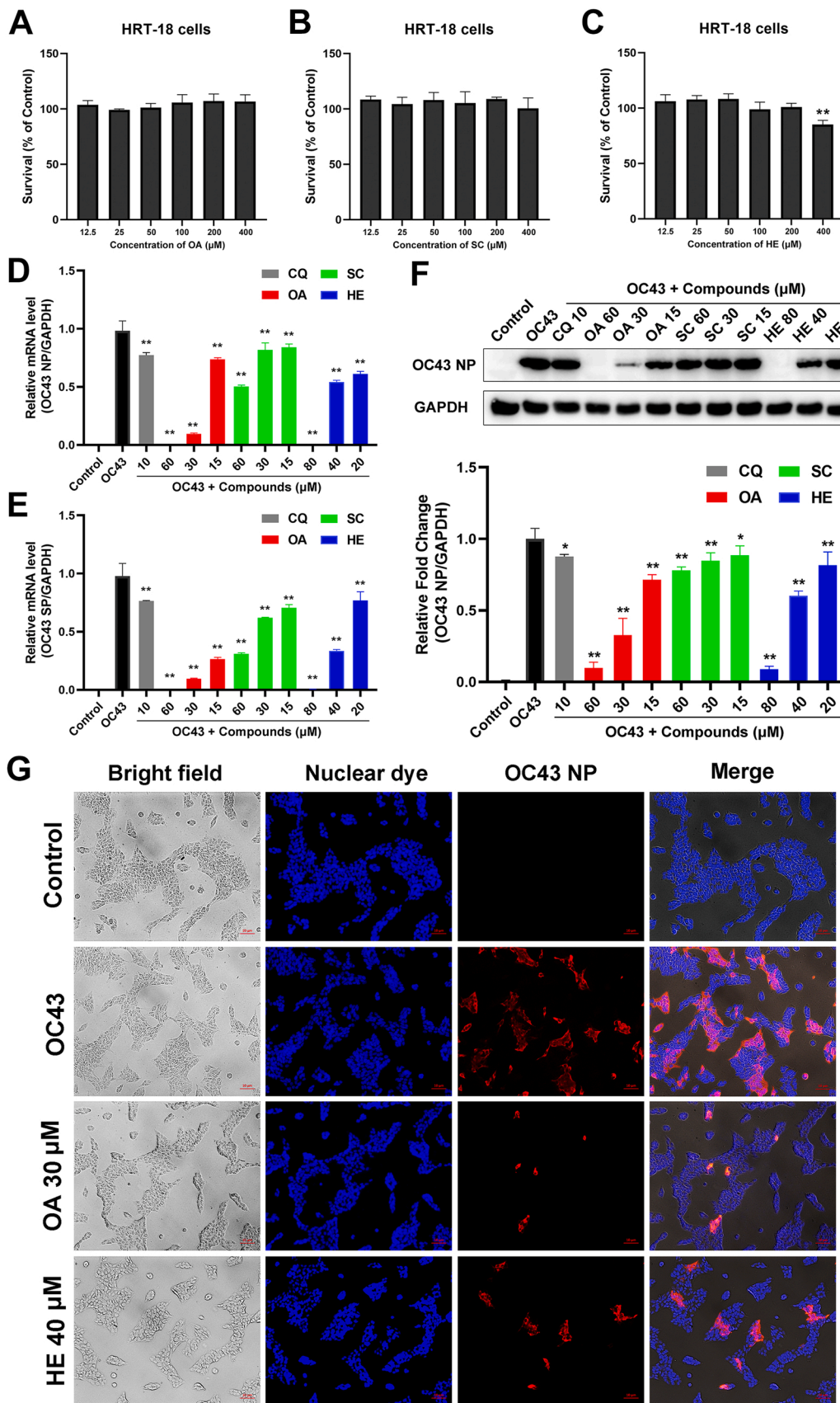


Fig. 8. Inhibitory activity of compounds against HCoV-OC43 infection in vitro. The cytotoxicity of OA (A), SC (B) and HE (C) towards HRT-18 cells was determined by CCK-8 assays. HCoV-OC43 NP (D) and SP (E) gene expression was analysed using quantitative RT-PCR with GAPDH as an internal control. (F) Expression of HCoV-OC43 NPs in HRT-18 cells was detected by western blot assay. CQ was used as a positive control. (G) HCoV-OC43 NP expression (red) was detected by indirect immunofluorescence assay. Nuclei (blue) were stained with DAPI, scale bar = 10 μm. The data are presented as the means ± SDs of triplicate samples from a representative experiment (**p*<0.05, ***p*<0.01).

Fig. 1 Data homogeneity diagram of the three microarray subdatasets included in this study.

Fig. 2 Effects of 10 high-degree compounds on IL-6 (A), CXCL-10 (B) and IL-1β (C) release from SARS-CoV-2 S protein-challenged THP-1 cells. The data are presented as the means ± SDs of triplicate samples from a representative experiment (**p*<0.05, ***p*<0.01, versus SARS-CoV-2 S protein).

Data analysis, Visualization. **Lin Li, Xiaoyan Pan:** Resources, Methodology and Supervision. All authors interpreted the results and critically revised the manuscript for scientific content. All authors approved the final version of the manuscript.

Conflict of interest statement

There are no known conflicts of interest associated with this publication and there has been no significant financial support for this work that could have influenced its outcome.

Availability of data and materials

The raw data supporting the conclusion of this article will be made available by the authors, without undue reservation, to any qualified researcher.

Appendix A. Supporting information

Supplementary data associated with this article can be found in the online version at [doi:10.1016/j.biopha.2022.113946](https://doi.org/10.1016/j.biopha.2022.113946).

References

- [1] P. Biswas, M.M. Hasan, D. Dey, A.C. Dos Santos Costa, S.A. Polish, S. Bibi, N. Ferdous, M.A. Kaium, M.H. Rahman, F.K. Jeet, S. Papadakos, K. Islam, M. S. Uddin, Candidate antiviral drugs for COVID-19 and their environmental implications: a comprehensive analysis, *Environ. Sci. Pollut. Res.* 28 (2021) 59570–59593.
- [2] A. Christie, J.T. Brooks, L.A. Hicks, E.K. Sauber-Schatz, J.S. Yoder, M.A. Honein, Guidance for implementing COVID-19 prevention strategies in the context of varying community transmission levels and vaccination coverage, *MMWR Morb. Mortal. Wkly Rep.* 70 (2021) 1044–1047.
- [3] P. Arora, C. Rocha, A. Kempf, I. Nehlmeier, L. Graichen, M.S. Winkler, M. Lier, S. Schulz, H.M. Jäck, A. Cossmann, M.V. Stankov, G. Behrens, S. Pöhlmann, M. Hoffmann, The spike protein of SARS-CoV-2 variant A.30 is heavily mutated and evades vaccine-induced antibodies with high efficiency, *Cell Mol. Immunol.* 18 (2021) 2673–2675.
- [4] P. Xie, Y. Fang, Z. Shen, Y. Shao, Q. Ma, Z. Yang, J. Zhao, H. Li, R. Li, S. Dong, W. Wen, X. Xia, Broad antiviral and anti-inflammatory activity of Qingwenjiere mixture against SARS-CoV-2 and other human coronavirus infections, *Phytomedicine* 93 (2021), 153808.
- [5] R. Yang, H. Liu, C. Bai, Y. Wang, X. Zhang, R. Guo, S. Wu, J. Wang, E. Leung, H. Chang, P. Li, T. Liu, Y. Wang, Chemical composition and pharmacological mechanism of Qingfei Paidu Decoction and Ma Xing Shi Gan Decoction against Coronavirus Disease 2019 (COVID-19): In silico and experimental study, *Pharm. Res* 157 (2020), 104820.
- [6] H. Luo, Q.L. Tang, Y.X. Shang, S.B. Liang, M. Yang, N. Robinson, J.P. Liu, Can Chinese medicine be used for prevention of corona virus disease 2019 (COVID-19)? a review of historical classics, research evidence and current prevention programs, *Chin. J. Integr. Med* 26 (2020) 243–250.
- [7] Q. Ma, W. Pan, R. Li, B. Liu, C. Li, Y. Xie, Z. Wang, J. Zhao, H. Jiang, J. Huang, Y. Shi, J. Dai, K. Zheng, X. Li, Z. Yang, Liu Shen capsule shows antiviral and anti-inflammatory abilities against novel coronavirus SARS-CoV-2 via suppression of NF- κ B signaling pathway, *Pharm. Res* 158 (2020), 104850.
- [8] D.Y.W. Lee, Q.Y. Li, J. Liu, T. Efferth, Traditional Chinese herbal medicine at the forefront battle against COVID-19: clinical experience and scientific basis, *Phytomedicine* 80 (2021), 153337.
- [9] F. Xu, T. Hou, A. Shen, H. Jin, Y. Xiao, W. Yu, X. Li, J. Wang, Y. Liu, X. Liang, Mechanism deconvolution of Qing Fei Pai Du decoction for treatment of Coronavirus Disease 2019 (COVID-19) by label-free integrative pharmacology assays, *J. Ethnopharmacol.* 280 (2021), 114488.
- [10] C. Wang, B. Cao, Q.Q. Liu, Z.Q. Zou, Z.A. Liang, L. Gu, J.P. Dong, L.R. Liang, X. W. Li, K. Hu, X.S. He, Y.H. Sun, Y. An, T. Yang, Z.X. Cao, Y.M. Guo, X.M. Wen, Y. G. Wang, Y.L. Liu, L.D. Jiang, Oseltamivir compared with the Chinese traditional therapy maxingshigan-yinqiaosan in the treatment of H1N1 influenza: a randomized trial, *Ann. Intern Med* 155 (2011) 217–225.
- [11] Q. Wang, H. Zhu, M. Li, Y. Liu, H. Lai, Q. Yang, X. Cao, L. Ge, Efficacy and safety of qingfei paidu decoction for treating COVID-19: a systematic review and meta-analysis, *Front Pharm.* 12 (2021), 688857.
- [12] W. Ren, Y. Ma, R. Wang, P. Liang, Q. Sun, Q. Pu, L. Dong, M. Mazhar, G. Luo, S. Yang, Research advance on qingfei paidu decoction in prescription principle, mechanism analysis and clinical application, *Front Pharm.* 11 (2021), 589714.
- [13] L. Zhang, X. Zheng, X. Bai, Q. Wang, B. Chen, H. Wang, J. Lu, S. Hu, X. Zhang, H. Zhang, J. Liu, Y. Shi, Z. Zhou, L. Gan, X. Li, J. Li, Association between use of Qingfei Paidu Tang and mortality in hospitalized patients with COVID-19: a national retrospective registry study, *Phytomedicine* 85 (2021), 153531.
- [14] N. Shi, B. Liu, N. Liang, Y. Ma, Y. Ge, H. Yi, H. Wo, H. Gu, Y. Kuang, S. Tang, Y. Zhao, L. Tong, S. Liu, C. Zhao, R. Chen, W. Bai, Y. Fan, Z. Shi, L. Li, J. Liu, H. Gu, Y. Zhi, Z. Wang, Y. Li, H. Li, J. Wang, L. Jiao, Y. Tian, Y. Xiong, R. Huo, X. Zhang, J. Bai, H. Chen, L. Chen, Q. Feng, T. Guo, Y. Hou, G. Hu, X. Hu, Y. Hu, J. Huang, Q. Huang, S. Huang, L. Ji, H. Jin, X. Lei, C. Li, G. Wu, J. Li, M. Li, Q. Li, X. Li, H. Liu, J. Liu, Z. Liu, Y. Ma, Y. Mao, L. Mo, H. Na, J. Wang, F. Song, S. Sun, D. Wang, M. Wang, X. Wang, Y. Wang, Y. Wang, W. Wu, L. Wu, Y. Xiao, H. Xie, H. Xu, S. Xu, R. Xue, C. Yang, K. Yang, P. Yang, S. Yuan, G. Zhang, J. Zhang, L. Zhang, S. Zhao, W. Zhao, K. Zheng, Y. Zhou, J. Zhu, T. Zhu, G. Li, W. Wang, H. Zhang, Y. Wang, Y. Wang, Association between early treatment with Qingfei Paidu decoction and favorable clinical outcomes in patients with COVID-19: a retrospective multicenter cohort study, *Pharm. Res* 161 (2020), 105290.
- [15] J. Zhao, S. Tian, D. Lu, J. Yang, H. Zeng, F. Zhang, D. Tu, G. Ge, Y. Zheng, T. Shi, X. Xu, S. Zhao, Y. Yang, W. Zhang, Systems pharmacological study illustrates the immune regulation, anti-infection, anti-inflammation, and multi-organ protection mechanism of Qing-Fei-Pai-Du decoction in the treatment of COVID-19, *Phytomedicine* 85 (2021), 153315.
- [16] W. Liu, J. Huang, F. Zhang, C. Zhang, R. Li, Y. Wang, C. Wang, X. Liang, W. Zhang, L. Yang, P. Liu, G. Ge, Comprehensive profiling and characterization of the absorbed components and metabolites in mice serum and tissues following oral administration of Qing-Fei-Pai-Du decoction by UHPLC-Q-Exactive-Orbitrap HRMS, *Chin J Nat, Medicines* 19 (2021) 305–320.
- [17] F. Islam, S. Bibi, A.F.K. Meem, M.M. Islam, M.S. Rahaman, S. Bepary, M. M. Rahman, M.M. Rahman, A. Elzaki, S. Kajoak, H. Osman, M. ElSamani, M. U. Khandaker, A.M. Idris, T.B. Emran, Natural Bioactive Molecules: An Alternative Approach to the Treatment and Control of COVID-19, *Int J. Mol. Sci.* 22 (2021) 12638.
- [18] S. Bibi, M.M. Hasan, Y.B. Wang, S.P. Papadakos, H. Yu, Cordycepin as a Promising Inhibitor of SARS-CoV-2 RNA Dependent RNA Polymerase (RdRp), *Curr. Med Chem.* 29 (2022) 152–162.
- [19] J. Fang, Q. Wu, F. Ye, C. Cai, L. Xu, Y. Gu, Q. Wang, A. Liu, W. Tan, G. Du, Network-Based Identification and Experimental Validation of Drug Candidates Toward SARS-CoV-2 via Targeting Virus–Host Interactome, *Front Genet* 12 (2021), 728960.
- [20] C. Shang, X. Zhuang, H. Zhang, Y. Li, Y. Zhu, J. Lu, C. Ge, J. Cong, T. Li, N. Li, M. Tian, N. Jin, X. Li, T. Gallagher, Inhibition of Autophagy Suppresses SARS-CoV-2 Replication and Ameliorates Pneumonia in hACE2 Transgenic Mice and Xenografted Human Lung Tissues, *J. Virol.* 95 (2021), e153721.
- [21] M. Hoffmann, H. Kleine-Weber, S. Pöhlmann, A. Multibasic, Cleavage site in the spike protein of SARS-CoV-2 is essential for infection of human lung cells, *Mol. Cell* 78 (2020) 779–784.
- [22] D. Blanco-Melo, B.E. Nilsson-Payant, W.C. Liu, S. Uhl, D. Hoagland, R. Moller, T. X. Jordan, K. Oishi, M. Panis, D. Sachs, T.T. Wang, R.E. Schwartz, J.K. Lim, R. A. Albrecht, B.R. TenOver, Imbalanced host response to SARS-CoV-2 drives development of COVID-19, *Cell* 181 (2020) 1036–1045.
- [23] N.A.P. Lieberman, V. Peddu, H. Xie, L. Shrestha, M. Huang, M.C. Mears, M. N. Cajimat, D.A. Bente, P. Shi, F. Bovier, P. Roychoudhury, K.R. Jerome, A. Moscona, M. Porotto, A.L. Greninger, In vivo antiviral host transcriptional response to SARS-CoV-2 by viral load, sex, and age, *Plos Biol.* 18 (2020), e3000849.
- [24] Z. Chen, Y. Sun, Q. Wang, H. Ma, Z. Ma, C. Yang, Integrated Analysis of Multiple Microarray Studies to Identify Novel Gene Signatures in Ulcerative Colitis, *Front Genet* 12 (2021), 697514.
- [25] T. Liang, J. Qiu, X. Niu, Q. Ma, C. Zhou, P. Chen, Q. Zhang, M. Chen, Z. Yang, S. Liu, L. Li, 3-Hydroxyphthalic Anhydride-Modified Chicken Ovalbumin as a Potential Candidate Inhibits SARS-CoV-2 Infection by Disrupting the Interaction of Spike Protein With Host ACE2 Receptor, *Front Pharm.* 11 (2021), 603830.
- [26] Y. Li, C. Yang, Y. Wu, J. Lv, X. Feng, X. Tian, Z. Zhou, X. Pan, S. Liu, L. Tian, Axial Chiral Binaphthoquinone and Perylenequinones from the Stromata of *Hyppocrella bambusae* Are SARS-CoV-2 Entry Inhibitors, *J. Nat. Prod.* 84 (2021) 436–443.
- [27] D. Dey, R. Hossain, P. Biswas, P. Paul, M.A. Islam, T.I. Ema, B.K. Gain, M.M. Hasan, S. Bibi, M.T. Islam, M.A. Rahman, B. Kim, Amentoflavone derivatives significantly act towards the main protease (3CLPRO/MPRO) of SARS-CoV-2: in silico admet profiling, molecular docking, molecular dynamics simulation, network pharmacology, *Mol. Divers* 31 (2022) 1–15.
- [28] Y. Li, X. Xie, S. Liao, Z. Zeng, S. Li, B. Xie, Q. Huang, H. Zhou, C. Zhou, J. Lin, Y. Huang, D. Xu, A011, a novel small-molecule ligand of σ 2 receptor, potently suppresses breast cancer progression via endoplasmic reticulum stress and autophagy, *Biomed. Pharm.* 152 (2022), 113232.
- [29] S. Kang, M. Yang, Z. Hong, L. Zhang, Z. Huang, X. Chen, S. He, Z. Zhou, Z. Zhou, Q. Chen, Y. Yan, C. Zhang, H. Shan, S. Chen, Crystal structure of SARS-CoV-2 nucleocapsid protein RNA binding domain reveals potential unique drug targeting sites, *Acta Pharm. Sin.* B 10 (2020) 1228–1238.
- [30] G. Song, X. Shen, S. Li, Y. Li, Y. Liu, Y. Zheng, R. Lin, J. Fan, H. Ye, S. Liu, Structure-activity relationships of 3-O- β -chacotriosyl ursolic acid derivatives as novel H5N1 entry inhibitors, *Eur. J. Med Chem.* 93 (2015) 431–442.
- [31] H. Li, C. Cheng, S. Li, Y. Wu, Z. Liu, M. Liu, J. Chen, Q. Zhong, X. Zhang, S. Liu, G. Song, Discovery and structural optimization of 3-O-beta-chacotriosyl oleanane-type triterpenoids as potent entry inhibitors of SARS-CoV-2 virus infections, *Eur. J. Med Chem.* 215 (2021), 113242.
- [32] J.R. Mascola, B.S. Graham, A.S. Fauci, SARS-CoV-2 Viral Variants-Tackling a Moving Target, *JAMA* 325 (2021) 1261–1262.
- [33] S. Xia, Y. Zhu, M. Liu, Q. Lan, W. Xu, Y. Wu, T. Ying, S. Liu, Z. Shi, S. Jiang, L. Lu, Fusion mechanism of 2019-nCoV and fusion inhibitors targeting HR1 domain in spike protein, *Cell Mol. Immunol.* 17 (2020) 765–767.
- [34] C. Yang, X. Pan, X. Xu, C. Cheng, Y. Huang, L. Li, S. Jiang, W. Xu, G. Xiao, S. Liu, Salvianolic acid C potently inhibits SARS-CoV-2 infection by blocking the

- formation of six-helix bundle core of spike protein, *Signal Transduct. Target Ther.* 5 (2020) 220.
- [35] S. Bibi, M.S. Khan, S.A. El-Kafrawy, T.A. Alandijany, M.M. El-Daly, Q. Yousafi, D. Fatima, A.A. Faizo, L.H. Bajrai, E.I. Azhar, Virtual screening and molecular dynamics simulation analysis of Forsythoside A as a plant-derived inhibitor of SARS-CoV-2 3CLpro, *Saudi. Pharm. J.* 30 (2022) 979–1002.
- [36] R. Yan, Y. Zhang, Y. Li, L. Xia, Y. Guo, Q. Zhou, Structural basis for the recognition of SARS-CoV-2 by full-length human ACE2, *Science* 367 (2020) 1444–1448.
- [37] S. Khan, M.S. Shafiei, C. Longoria, J.W. Schoggins, R.C. Savani, H. Zaki, SARS-CoV-2 spike protein induces inflammation via TLR2-dependent activation of the NF- κ B pathway, *Elife* 10 (2021), e68563.
- [38] M. Zheng, R. Karki, E.P. Williams, D. Yang, E. Fitzpatrick, P. Vogel, C.B. Jonsson, T. D. Kanneganti, TLR2 senses the SARS-CoV-2 envelope protein to produce inflammatory cytokines, *Nat. Immunol.* 22 (2021) 829–838.
- [39] R. Zhou, L. Liu, Y. Wang, Viral proteins recognized by different TLRs, *J. Med Virol.* 93 (2021) 6116–6123.
- [40] A.E. Peter, B.V. Sandeep, B.G. Rao, V.L. Kalpana, Calming the storm: natural immunosuppressants as adjuvants to target the cytokine storm in COVID-19, *Front Pharm.* 11 (2020), 583777.
- [41] A. Gour, D. Manhas, S. Bag, B. Gorain, U. Nandi, Flavonoids as potential phytotherapeutics to combat cytokine storm in SARS-CoV-2, *Phytother. Res* 35 (2021) 4258–4283.
- [42] K. Owczarek, A. Szczepanski, A. Milewska, Z. Baster, Z. Rajfur, M. Sarna, K. Pyrc, Early events during human coronavirus OC43 entry to the cell, *Sci. Rep.* 8 (2018) 7124.
- [43] X. Zong, N. Liang, J. Wang, H. Li, D. Wang, Y. Chen, H. Zhang, L. Jiao, A. Li, G. Wu, J. Li, M. Wang, H. Liu, Z. Liu, S. Zhao, J. Huang, Q. Huang, X. Wang, J. Qin, Y. Ma, Y. Wang, N. Shi, Treatment Effect of Qingfei Paidu Decoction Combined With Conventional Treatment on COVID-19 Patients and Other Respiratory Diseases: A Multi-Center Retrospective Case Series, *Front Pharm.* 13 (2022), 849598.
- [44] B. Kwon, J. Song, H. Song, J.W. Kang, S.N. Hwang, K. Rhee, A. Shim, E. Hong, Y. Kim, S. Jeon, S. Chang, D. Kim, S. Cho, H. Ko, Antiviral Activity of Oroxylin A against Coxsackievirus B3 Alleviates Virus-Induced Acute Pancreatic Damage in Mice, *Plos One* 11 (2016), e155784.
- [45] H.J. Choi, H.H. Song, J.S. Lee, H.J. Ko, J.H. Song, Inhibitory Effects of Norwogonin, Oroxylin A, and Mosloflavone on Enterovirus 71, *Biomol. Ther. (Seoul.)* 24 (2016) 552–558.
- [46] S. Ma, J. Du, P. Pui-Hay But, X. Deng, Y. Zhang, V. Eng-Choon Ool, H. Xu, S. Hon-Sun Lee, S.F. Lee, Antiviral chinese medicinal herbs against respiratory syncytial virus, *J Ethnopharmacol* 79 (2002) 205–211.
- [47] J. Jin, S. Chen, D. Wang, Y. Chen, Y. Wang, M. Guo, C. Zhou, J. Dou, Oroxylin A suppresses influenza A virus replication correlating with neuraminidase inhibition and induction of IFNs, *Biomed. Pharm.* 97 (2018) 385–394.
- [48] J. Gao, Y. Ding, Y. Wang, P. Liang, L. Zhang, R. Liu, Oroxylin A is a severe acute respiratory syndrome coronavirus 2–spiked pseudotyped virus blocker obtained from Radix Scutellariae using angiotensin-converting enzymell/cell membrane chromatography, *Phytother. Res* 35 (2021) 3194–3204.
- [49] J.S. Min, D.E. Kim, Y. Jin, S. Kwon, Kurarinone inhibits HCoV-OC43 infection by impairing the virus-induced autophagic flux in MRC-5 Human Lung Cells, *J. Clin. Med* 9 (2020) 2230.
- [50] C. Li, L. Zhang, G. Lin, Z. Zuo, Identification and quantification of baicalain, wogonin, oroxylin A and their major glucuronide conjugated metabolites in rat plasma after oral administration of Radix scutellariae product, *J. Pharm. Biomed.* 54 (2011) 750–758.
- [51] L. Koepke, M. Hirschenberger, M. Hayn, F. Kirchhoff, K.M. Sparrer, Manipulation of autophagy by SARS-CoV-2 proteins, *Autophagy* 17 (2021) 2659–2661.
- [52] W. Twu, J. Lee, H. Kim, V. Prasad, B. Cerikan, U. Haselmann, K. Tabata, R. Bartenschlager, Contribution of autophagy machinery factors to HCV and SARS-CoV-2 replication organelle formation, *Cell Rep.* 37 (2021), 110049.
- [53] R. Huang, M. Xu, H. Zhu, C.Z. Chen, W. Zhu, E.M. Lee, S. He, L. Zhang, J. Zhao, K. Shamim, D. Bougie, W. Huang, M. Xia, M.D. Hall, D. Lo, A. Simeonov, C. P. Austin, X. Qiu, H. Tang, W. Zheng, Biological activity-based modeling identifies antiviral leads against SARS-CoV-2, *Nat. Biotechnol.* 39 (2021) 747–753.
- [54] J. Yao, J. Wang, Y. Xu, Q. Guo, Y. Sun, J. Liu, S. Li, Y. Guo, L. Wei, CDK9 inhibition blocks the initiation of PINK1-PRKN-mediated mitophagy by regulating the SIRT1-FOXO3-BNIP3 axis and enhances the therapeutic effects involving mitochondrial dysfunction in hepatocellular carcinoma, *Autophagy* 18 (2021) 1–19.
- [55] F. Cheng, T. Huynh, C. Yang, D. Hu, Y. Shen, C. Tu, Y. Wu, C. Tang, W. Huang, Y. Chen, C. Ho, Hesperidin Is a Potential Inhibitor against SARS-CoV-2 Infection, *Nutrients* 13 (2021) 2800.
- [56] H.O. GÜLER, F. AY ŞAL, Z. CAN, Y. KARA, O. YILDIZ, A.O. BELDÜZ, S. ÇANAKÇI, S. KOLAYLI, Targeting CoV-2 spike RBD and ACE-2 interaction with flavonoids of Anatolian propolis by in silico and in vitro studies in terms of possible COVID-19 therapeutics, *Turk. J. Biol.* 45 (2021) 530–548.
- [57] R. Ghosh, A. Chakraborty, A. Biswas, S. Chowdhuri, Depicting the inhibitory potential of polyphenols from *Isatis indigotica* root against the main protease of SARS CoV-2 using computational approaches, *J. Biomol. Struct. Dyn.* 40 (2020) 1–12.
- [58] A. Kandeil, A. Mostafa, O. Kutkat, Y. Moatasim, A.A. Al-Karmalawy, A.A. Rashad, A.E. Kayed, A.E. Kayed, R. El-Shesheny, G. Kayali, M.A. Ali, Bioactive Polyphenolic Compounds Showing Strong Antiviral Activities against Severe Acute Respiratory Syndrome Coronavirus 2, *Pathogens* 10 (2021) 758.
- [59] X. Wang, H. Xia, Y. Liu, F. Qiu, X. Di, Simultaneous determination of three glucuronide conjugates of scutellarein in rat plasma by LC-MS/MS for pharmacokinetic study of breviscapine, *J. Chromatogr. B* 965 (2014) 79–84.
- [60] X. Tian, L. Chang, G. Ma, T. Wang, M. Lv, Z. Wang, L. Chen, Y. Wang, X. Gao, Y. Zhu, S.K.L.O. ATianjin, A.B.P.C. Present, A.T.F.T. Present, U.O.T.C. Tianjin, A.D. C.O. BResearch, Ltd, I.J.A.O. Tianjin, C.R.I. CMolecular, M.C. Tufts, Delineation of Platelet Activation Pathway of Scutellarein Revealed Its Intracellular Target as Protein Kinase C, *Biol. Pharm. Bull.* 39 (2016) 181–191.
- [61] J. Cheng, N. Sun, X. Zhao, L. Niu, M. Song, Y. Sun, J. Jiang, J. Guo, Y. Bai, J. He, H. Li, In vitro screening for compounds derived from traditional chinese medicines with antiviral activities against porcine reproductive and respiratory syndrome virus, *J. Microbiol. Biotechnol.* 23 (2013) 1076–1083.
- [62] G. Zhang, Q. Wang, J. Chen, X. Zhang, S. Tam, Y. Zheng, The anti-HIV-1 effect of scutellarin, *Biochem Bioph Res Co.* 334 (2005) 812–816.
- [63] H. Liu, F. Ye, Q. Sun, H. Liang, C. Li, S. Li, R. Lu, B. Huang, W. Tan, L. Lai, Scutellaria baicalensis extract and baicalin inhibit replication of SARS-CoV-2 and its 3C-like protease in vitro, *J. Enzym. Inhib. Med Chem.* 36 (2021) 497–503.
- [64] H.X. Su, S. Yao, W.F. Zhao, M.J. Li, J. Liu, W.J. Shang, H. Xie, C.Q. Ke, H.C. Hu, M. N. Gao, K.Q. Yu, H. Liu, J.S. Shen, W. Tang, L.K. Zhang, G.F. Xiao, L. Ni, D. W. Wang, J.P. Zuo, H.L. Jiang, F. Bai, Y. Wu, Y. Ye, Y.C. Xu, Anti-SARS-CoV-2 activities in vitro of Shuanghuanglian preparations and bioactive ingredients, *Acta Pharm. Sin.* 41 (2020) 1167–1177.
- [65] P.M. George, A.U. Wells, R.G. Jenkins, Pulmonary fibrosis and COVID-19: the potential role for antifibrotic therapy, *Lancet Respir Med* 8 (2020) 807–815.
- [66] Y. Wu, L. Xu, G. Cao, L. Min, T. Dong, Effect and Mechanism of Qingfei Paidu Decoction in the Management of Pulmonary Fibrosis and COVID-19, *Am. J. Chin. Med* 50 (2022) 33–51.
- [67] J. Shimizu, T. Sasaki, A. Yamanaka, Y. Ichihara, R. Koketsu, Y. Samune, P. Cruz, K. Sato, N. Tanga, Y. Yoshimura, A. Murakami, M. Yamada, K. Itoi, E.E. Nakayama, K. Miyazaki, T. Shioda, The potential of COVID-19 patients' sera to cause antibody-dependent enhancement of infection and IL-6 production, *Sci. Rep.* 11 (2021) 23713.
- [68] P. Asrani, M.I. Hassan, SARS-CoV-2 mediated lung inflammatory responses in host: targeting the cytokine storm for therapeutic interventions, *Mol. Cell Biochem* 476 (2021) 675–687.
- [69] C.F. Hsieh, C.W. Lo, C.H. Liu, S. Lin, H.R. Yen, T.Y. Lin, J.T. Horng, Mechanism by which ma-xing-shi-gan-tang inhibits the entry of influenza virus, *J. Ethnopharmacol.* 143 (2012) 57–67.
- [70] C.C. Lin, Y.Y. Wang, S.M. Chen, Y.T. Liu, J.Q. Li, F. Li, J.C. Dai, T. Zhang, F. Qiu, H. Liu, Z. Dai, Z.D. Zhang, Shegan-Mahuang Decoction ameliorates asthmatic airway hyperresponsiveness by downregulating Th2/Th17 cells but upregulating CD4⁺FoxP3⁺ Tregs, *J. Ethnopharmacol.* 253 (2020), 112656.
- [71] P.W. Cheng, L.T. Ng, C.C. Lin, Xiao chai hu tang inhibits CVB1 virus infection of CCFPS-1 cells through the induction of Type I interferon expression, *Int Immunopharmacol.* 6 (2006) 1003–1012.
- [72] J. Chen, Y.K. Wang, Y. Gao, L.S. Hu, J.W. Yang, J.R. Wang, W.J. Sun, Z.Q. Liang, Y. M. Cao, Y.B. Cao, Protection against COVID-19 injury by qingfei paidu decoction via anti-viral, anti-inflammatory activity and metabolic programming, *Biomed. Pharm.* 129 (2020), 110281.
- [73] S. Jia, H. Luo, X. Liu, X. Fan, Z. Huang, S. Lu, L. Shen, S. Guo, Y. Liu, Z. Wang, L. Cao, Z. Cao, X. Zhang, W. Zhou, J. Zhang, J. Li, J. Wu, W. Xiao, Dissecting the novel mechanism of reduning injection in treating Coronavirus Disease 2019 (COVID-19) based on network pharmacology and experimental verification, *J. Ethnopharmacol.* 273 (2021), 113871.
- [74] Q. Ma, Z. Wang, R. Chen, B. Lei, B. Liu, H. Jiang, Z. Chen, X. Cai, X. Guo, M. Zhou, J. Huang, X. Li, J. Dai, Z. Yang, Effect of Jinzhen granule on two coronaviruses: The novel SARS-CoV-2 and the HCoV-229E and the evidences for their mechanisms of action, *Phytomedicine* 95 (2022), 153874.
- [75] H. Lin, X. Wang, M. Liu, M. Huang, Z. Shen, J. Feng, H. Yang, Z. Li, J. Gao, X. Ye, Exploring the treatment of COVID-19 with Qingqiao powder based on network pharmacology, *Phytother. Res* 35 (2021) 2651–2664.
- [76] X. Chen, Y. Wu, C. Chen, Y. Gu, C. Zhu, S. Wang, J. Chen, L. Zhang, L. Lv, G. Zhang, Y. Yuan, Y. Chai, M. Zhu, C. Wu, Identifying potential anti-COVID-19 pharmacological components of traditional Chinese medicine Lianhuaqingwen capsule based on human exposure and ACE2 biochromatography screening, *Acta Pharm. Sin. B* 11 (2021) 222–236.